

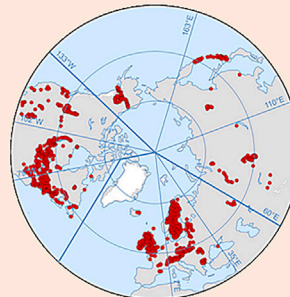
Article

The ghost of ice ages past: Impact of Last Glacial Maximum landscapes on modern biodiversity

What: 47 micro land-snail species of three genera

Where: Holarctic (8,900 records)

When: From LGM (21 ka) to today



Modelling of distribution ranges in LGM & today

Including LGM fossils improved model quality
Ice sheets are periodic barriers as effective as oceans

21 ka (LGM)



**barrier width
reduced by 50%**



**species ranges
doubled in size**

Today



Jeffrey C. Nekola,
Jan Divíšek, Michal
Horsák

horsak@sci.muni.cz

Highlights

First global range modeling exercise, including fossils, for multiple species

Potential modern ranges are unsaturated due to past and current barriers

Landscape template over 15 ka helps to explain current biodiversity

Nekola et al., iScience 27, 111272
December 20, 2024 © 2024 The Author(s). Published by Elsevier Inc.
<https://doi.org/10.1016/j.isci.2024.111272>



Article

The ghost of ice ages past: Impact of Last Glacial Maximum landscapes on modern biodiversity

Jeffrey C. Nekola,¹ Jan Divíšek,¹ and Michal Horsák^{1,2,*}

SUMMARY

Modeled modern and Last Glacial Maximum (LGM) climate ranges for 47 genetically confirmed small Holarctic land snails documented profound landscape dynamism over the last 21,000 years. Following deglaciation, range areas tended to increase by 50% while isolating barrier widths were cut in half. At the same time, the nature of isolating barriers underwent profound change, with the North American continental ice sheet becoming as important in the LGM as the Atlantic Ocean is today in separating Nearctic and Palearctic faunas. Because appropriate modern climate occurs for these species throughout the Holarctic, with no clear barriers being present—especially for such efficient passive dispersers—the current >90% turnover observed between Eurasian and North American species pools appears at least in part related to the LGM landscape. Understanding current and predicting potential future biodiversity patterns thus requires consideration of the landscape template across at least 15,000 years time scales.

INTRODUCTION

Biodiversity is more than just the total number of species; it also reflects assemblage variability. Also called “turnover”, “beta-diversity”, or “distance decay”,¹ this factor allows areas to be unique not only in terms of their species composition but also potential ecological interactions.² Two main non-biological drivers generate turnover: environmental variation and the geographic template of habitat occurrence. Documenting how these contribute to biotic uniqueness is essential to understanding the mechanisms responsible for global biodiversity.³

For instance, regional land snail species pool composition changes by over 95% across the Holarctic from Western Europe to eastern North America. However, this turnover is not related to climate because potential species ranges reflecting only appropriate climate generally have global coverage.⁴ Given that soil and water conditions are found throughout, the uniqueness of regional boreal land snail faunas appears to be related to dispersal barriers, which keep species confined to a subset of their potential global range. However, more than current barriers may be at play; for instance, North American species are absent from adjacent eastern and central Asia even though more potential appropriate climate actually exists for them there. Likewise, a number of central and eastern Asian species are absent from North America in spite of the presence of appropriate climate. Yet, <200 km of ocean or climate barriers is all that currently separates these faunas.⁴

It appears that current biodiversity may reflect more than modern conditions. Ranges and barriers may be in flux given that the atmosphere demonstrates constant variability across all temporal and spatial scales.⁵ Climate has been especially variable over the last 3 million years, where at least 30 periods of extreme cold (each lasting up to 100 ka) have been punctuated by shorter (~15 ka) intervals of relative warmth.⁶ At the end of the Last Glacial Maximum (LGM), continental ice sheets rapidly retreated in the face of climate change⁷ and eventually collapsed across both northern Europe and North America. LGM paleoecological reconstructions suggest not only that continental ice sheets could have served as a barrier to biological movement⁸ but also that tundra, taiga, and temperate forest became compressed into what are now temperate latitudes.⁹ There is thus no reason to expect that modern biodiversity will reflect only current landscape conditions.¹⁰

Here, we advance understanding of species range and barrier dynamics since the LGM and consider how this has influenced modern biodiversity. We do this by documenting differences in potential modern and LGM ranges and dispersal barriers using Maxent climate envelopes individually fit for 47 genetically validated boreal land snail species using over 8,900 confirmed occurrences across the Holarctic (Figure 1A). These were calibrated either from modern (unitemporal models) or both modern and LGM occurrences (multitemporal models). Each species envelope was then projected into the modern and an ensemble of predicted LGM climate landscapes, with basic range/barrier attributes being measured and statistically compared across nine Holarctic regions of roughly similar latitudinal extent (Figure 1B).

These species represent an ideal system in which study the ecological and biogeographic impacts of climatically induced global-scale range and barrier dynamism because: (1) they collectively occur throughout the Holarctic, where they represent about 10% of the entire modern small-sized fauna¹¹; (2) they are among the most abundant modern boreal land snails, occurring across all habitat types and trophic

¹Department of Botany and Zoology, Faculty of Science, Masaryk University, Kotlářská 2, CZ-61137 Brno, Czech Republic

²Lead contact

*Correspondence: horsak@sci.muni.cz
<https://doi.org/10.1016/j.isci.2024.111272>



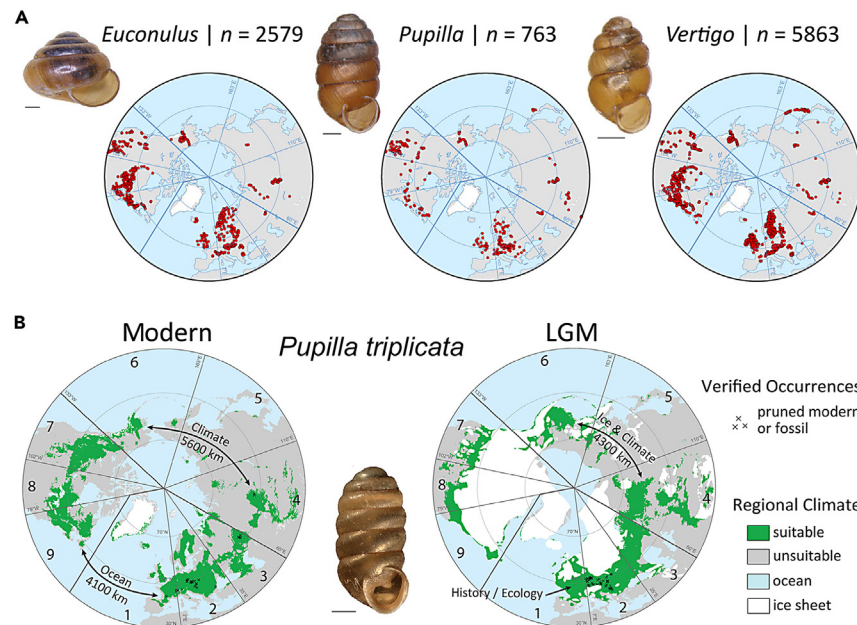


Figure 1. Sample data and example range/barrier projection

(A) Sample locations used to parameterize climate niche models across all species within each genus, with representative species from each is illustrated (scale bar, 0.5 mm).

(B) Range and barrier analysis for *Pupilla triplicata*. The predicted potential range (green) is based on 51 verified populations across the entire known range in addition to 51 quasi-occurrences within its LGM fossil range. In modern this species is known from regions 1–4, with LGM fossils being limited to region 2. Its total potential range across all regions is projected to be 8.0 million km² and was 4.9 million km² during the LGM. If dispersal barriers were absent, it is also projected to occur in regions 6–9 in both the LGM and modern. The modern occupied range is separated by 4,100 km of ocean from nearest suitable climate in Newfoundland, while the eastern range limit is separated by 5,600 km of inappropriate climate from the nearest suitable climate in SW Alaska. In the LGM the predicted western range limit was separated by a 3,600 km ocean barrier from the nearest appropriate climate in the exposed continental shelf off of Newfoundland, while the predicted eastern range limit was separated by 6,100 km of ice and inappropriate climate from the nearest appropriate climate on the exposed continental shelf off of SW Alaska.

states^{12,13}; (3) they possess one of the most abundant and extensive Pleistocene fossil records of any invertebrate group, being found in thousands of deposits across the Holarctic^{14,15}; (4) global phylogenies created from mitochondrial DNA (mtDNA) and nuclear DNA (nDNA) sequences document that all modeled entities represent highly supported species-level clades^{16–18} that possess diagnostic shell features allowing for accurate identification. They also exhibit no phylogenetic autocorrelation in observed or modeled ranges in either the modern or LGM (Table 1). The findings presented here can thus be considered independent of phylogeny; (5) while small land snails are among the most effective known passive dispersers, with multiple ocean crossings of 7,500 km having been documented,^{19,20} strong climatically uncorrelated turnover exists in their Holarctic regional species pools,⁴ suggesting the presence of additional drivers; and (6) in spite of decades of attempts to document competitive exclusion in land snails, this has never been shown.²¹ As a result, their occurrences are biologically independent²² and likely to be underlain by the physical environment only.

RESULTS

Range modeling accuracy

Cross-validation statistics for modern and LGM climatic range projections for all taxa (Data S1), showed that each unitemporal Maxent climate envelope adequately portrayed their respective modern occurrences (Data S2). Although 16 of 18 multitemporal models for species possessing LGM occurrence data generated higher Boyce evaluation scores for fossil occurrences than their corresponding unitemporal models, we note that their range and barrier central tendencies and distribution shapes were fundamentally similar to their unitemporal models (Table S1; Figures S1 and S2). Because both approaches thus appear to similarly document dynamics, we have chosen to include species lacking a fossil record by projecting their unitemporal envelopes into the LGM landscape. This allows for consideration of common taiga species lacking fossils due their limitation to acidic soils,²³ thereby allowing for a broader consensus and improved statistical power.

LGM-to-modern range and barrier dynamics

Change in total occupied range area varied from a ~50% reduction to 4× increase, with the median response representing a 42% increase (Figure 2; Table S2, Data S1 and S3). Seventy-percent of species (33 of 47) increased their total range area following deglaciation. This tendency was statistically significant (Figure 2A, $p < 0.001$). Potential range area within occupied biogeographic regions varied from a

Table 1. The results of the Mantel tests indicating no phylogenetically driven spatial autocorrelation in the observed and modeled species ranges in the LGM and Modern periods

	Modern	LGM
Observed distribution	$r = -0.028, p = 0.762$	N/A
Modelled distribution		
"Raw" occupancy of the biogeographical regions (km ²)	$r = 0.045, p = 0.296$	$r = -0.012, p = 0.5$
Relative occupancy of the biogeographical regions (%)	$r = 0.012, p = 0.429$	$r = -0.028, p = 0.615$

The Mantel statistics (r) shows the relationship between the pairwise dissimilarity of the species distributions and the phylogenetic distance of each pair of species. Positive values indicate a phylogenetic signal. The statistical significance of r was tested with 999 permutations.

94% reduction to 100× increase, with the median response representing a 23% increase. Fifty-five percent of the largest contiguous appropriate climate patches within regions (83 of 149) exhibited an increase following deglaciation (Figure 2B). This tendency was also highly significant ($p < 0.001$). Change in potential range area significantly varied between regions (Figure 3A, $p < 0.001$) being roughly constant in western Europe (region 1) and central/eastern Beringia (regions 5 and 6) but approximately doubling—with at least an additional 10⁶ km² per species—in North America (regions 7–9). The percent of total modern range overlapping LGM range significantly varied among the three different biogeographic groups (Figure 3B, $p \ll 0.001$), being the highest for Beringian species (median = 47%), followed by European (23%) and North American (13%). Among biogeographic regions, median overlap ranged from 43 to 67% in Beringia, 23–37% in Europe, and 0.3–12% in North America (Figure 3, Data S3). These differences were highly significant ($p \ll 0.001$). The proportion of species exhibiting complete range displacement between LGM and modern also significantly varied (Table 2A), being least frequent within Beringian regional species pools (0–13%) and most common in central and eastern North America (67–94%). In these last two regions the minimum movement required for species to track their shifting climate generally ranged between 100 and 900 km with a median of 300 km (Data S4).

Change in width for the 60 barriers persisting from the LGM to modern (e.g., lacking a historical/ecological range limit in either time period) varied from a 90% reduction to a 2.6× increase, with median response representing a 53% reduction—or 1,250 km (Figure 2, Data S1 and S4). In all, 48 barriers (80%) decreased in width following deglaciation. The factors generating barriers also significantly differed (Table 2B, $p \ll 0.001$) with there being an almost 60% increase in the frequency of history/ecology range limits in the modern. Because this may be due to the simple fact that such boundaries are more difficult to identify in the LGM due to incompleteness of the fossil and environmental record, we repeated the analyses following removal of this category. The results remained highly significant ($p < 0.001$) with a 7× increase in ice barrier frequency during the LGM. No significant difference ($p = 0.301$) was observed in the relative frequency of ocean and climate barriers from LGM to modern. While barrier type frequency did not change for European species ($p = 0.664$), both Beringian ($p = 0.006$) and North American ($p < 0.001$) species experienced a highly significant enrichment in ice barriers during the LGM (Table 2C).

The impact of former barriers, mainly LGM continental ice sheets, has had a profound impact on modern biodiversity (Figure 4). While appropriate climate for European, Beringian, and North American species occurs across the entire Holarctic, past and present climate and ice barriers have kept European species from colonizing regions east of central Asia, while the North American ice sheet was effective in preventing wholesale mixing of the North American and Beringian faunas. This has led to the reduction in regional species pool size while creating considerable compositional turnover between them.

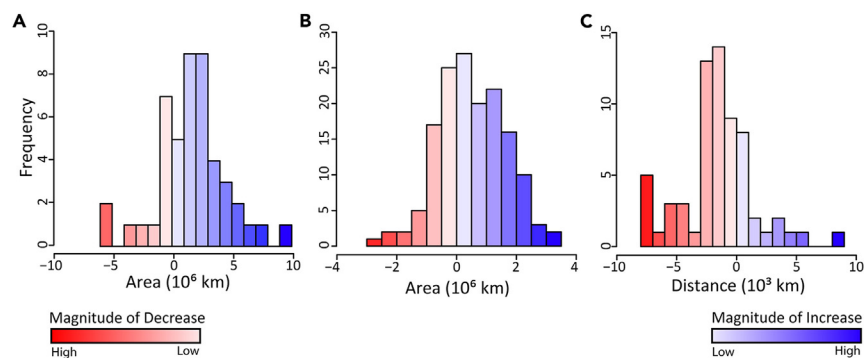


Figure 2. Pairwise change from LGM to modern

Comparison of (A) potential global range area (B) maximum patch size per biogeographic region and (C) barrier widths. Differences are tested based on paired Wilcoxon signed rank test and are significant at $p < 0.001$.

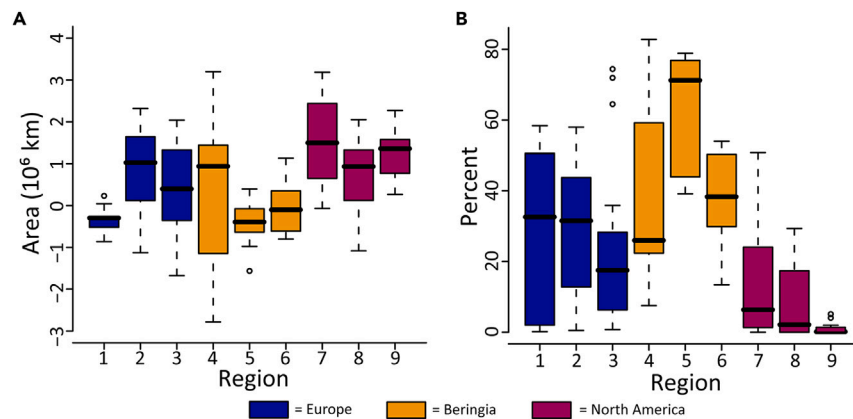


Figure 3. Change from LGM to modern

Comparison of (A) range size and (B) modern range overlap with LGM range for all taxa within biogeographic regions. Differences between three regions are based on Kruskal-Wallis test estimating the likelihood that group medians are the same. The central line of each box refers to the median value, box height to the interquartile range, whiskers to the non-outlier range (i.e. 1.5 times the interquartile range), and circle to an outlier. The differences are significant at $p \ll 0.001$.

DISCUSSION

These results not only document a profound change in the Holarctic biogeographic template from the LGM to modern but also help clarify the mechanisms underlying development and maintenance of its biodiversity. Three outcomes are of particular interest: First is the smaller range size and increased barrier distance for most taxa in the LGM vs. modern. This replicates similar projections generated over the same time period for forest trees⁹ and migratory birds.⁸ Reductions in range size and increases in isolation could also underlie frequent Pleistocene-aged phylogenesis seen in the time-calibrated global *Vertigo* tree.²⁰ They may also have contributed to modern intraspecific gene pool diversity: For instance, *Vertigo microsphaera* contains three to four distinct, well-supported clades in both nDNA and mtDNA. Their coexistence

Table 2. Comparison of ranges and barriers between LGM and Modern

A	Biogeographical region								
Ranges	1	2	3	4	5	6	7	8	9
Overlapping	12	13	14	15	11	16	12	6	1
Segregated	6	5	4	2	0	0	4	12	16
Log Likelihood test: $p \ll 0.001$									
B	LGM				Modern				
Barrier type	C	O	I	H	–	C	O	I	H
Count	30	45	4	29	–	31	31	34	18
Fisher's exact for LGM vs. Modern: $p \ll 0.001$									
Fisher's exact excluding H: $p < 0.001$									
Fisher's exact excluding I and H: $p = 0.301$									
C	LGM				Modern				
Affinity:	C	O	I	–	C	O	I	–	–
European	12	13	4	–	12	11	7	–	–
Beringian	8	8	0	–	8	6	10	–	–
North American	10	24	0	–	11	14	17	–	–
Fisher's exact LGM vs. modern:									
European, $p = 0.664$; Beringian, $p = 0.006$; North American, $p < 0.001$									

(A) Number of species with overlapping or segregated LGM vs. modern ranges in each region

(B) Frequency of LGM vs. modern barrier type counted across all species

(C) Frequency of LGM vs. modern barrier type counted across biogeographic affinity groups. Biogeographic region numbers correspond to Figure 1B. Barrier type codes represent: C = Inappropriate Climate; O = Ocean; I = Ice Sheet; H = Habitat/History where range terminates at least 1,500 km prior to end of modeled appropriate climate.

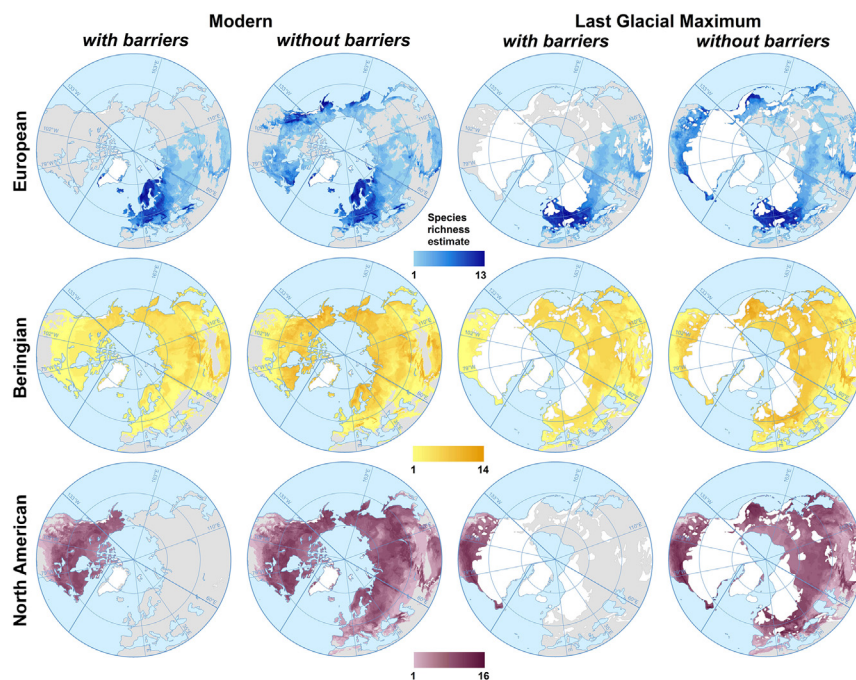


Figure 4. Estimated consensus richness of European, Beringian, and North American species for Modern and LGM Holarctic landscapes

In both time periods, “with barriers” represents the summation of predicted ranges only from biogeographic regions that have actually supported each species. “Without barriers” represents the total Holarctic sum of predicted ranges based only on climate. Note that we have not included in the “Modern - with barriers” map the two European species translocated to North America by humans over the last 500 years (*Pupilla muscorum* and *Vertigo pygmaea*).

within single populations possessing uniform shells with independent sorting of nDNA and mtDNA clade membership among individuals indicates that only a single biological species is present.¹⁷ Interestingly, the LGM range projection for this species suggests the presence of at least three roughly discrete subpopulations centered on southern Alaska, Japan/mainland East Asia, and the interior mountain ranges of central Asia (Figure S1). Such a general correspondence between the number of modern intraspecific genetic clades and discrete modeled LGM subpopulations is replicated in *Euconulus alderi*, *E. fulvus*, *Pupilla alpicola*, *V. alpestris*, *V. columbiana*, *V. kushiroensis*, and *V. lilljeborgi*.^{16–18} Similar patterns are also present in other boreal species groups—including orthopterans, birds, mammals, amphibians and vascular plants—which have experienced elevated rates of Pleistocene-era diversification.^{24–27} The conclusion that ice-age climate fluctuations have not significantly contributed to diversification,²⁸ thus seems at least partially driven by a focus on mid-to low-latitude species whose landscape template may have been more stable.

Second is the importance of former dispersal barriers in generating uniqueness between modern faunas. While dispersal limitation due to the north Atlantic Ocean and dry central Asian climates is not surprising, the former North American LGM continental ice sheet also appears to have left an indelible mark on modern biogeography in spite of the fact that it ceased to exist ~14 ka BP.²⁹ The simplest explanation for the absence of common North American boreal taxa (e.g., *Euconulus fresti*, *Pupilla hudsonianum*, and *Vertigo modesta*) from central and eastern Asia—which supports abundant potential climate and habitat—is this former ~2,000 km frozen ocean which once separated the North American tundra/taiga from Beringia (Figure 4). Concomitantly, a number of Beringian taxa (e.g., *Pupilla alaskensis* and *Vertigo beringiana*) appear to have been limited in their eastward expansion into appropriate boreal North America climates and habitats by this same feature. If well-mixed, central and eastern Beringian and central and eastern North American faunas should be at least 80% similar; instead their actual overlap is <10%.⁴ Clearly modern ranges are not in equilibrium with climate, with this ancient barrier having apparently contributed to the 100× greater observed turnover rates. It remains unanswered, however, how the more recent, <200-km wide Bering Strait ocean barrier should be so effective at inhibiting current westward movement, especially for efficient passive dispersers such as these small snails.¹⁹ Additional research on this topic is therefore necessary.

Lastly, we note in passing that there is little evidence to suggest that regional species richness is correlated with landscape stability: The Holarctic region with the most stable ranges—central Beringia, where over 2/3 of modern ranges area overlaps LGM ranges and where no species experienced complete LGM-to-modern latitudinal range segregation—has the smallest species pool ($n = 11$). However, central and eastern North America—which had the most dynamic ranges with <20% overlap between modern and LGM ranges and 67–94% of species having complete LGM-to-modern latitudinal range segregation—were tied for the richest ($n = 17$ and 18). The minimum northward distances these North American species were required to move to remain within their climate zone roughly equates to 1/3 or more of their modern latitudinal range.⁴ This surprising result may be related to the high passive dispersal ability of small land snails,¹⁹ which not only enabled their transcontinental dispersal over evolutionary time scales²⁰ but should permit rapid response to climate change—perhaps via bird migration

pathways.⁸ However, intraspecific genetic diversity does appear higher within Beringian vs. central/eastern North American species,^{16–18} suggesting that environmental stability may contribute to gene-pool biodiversity.

These findings represent a profound reminder that current biodiversity and biogeographic patterns should not be solely interpreted from current conditions, as is often documented at regional scales.³⁰ Our global analyses suggest that modern Holarctic biodiversity has been enriched by the presence of a long-vanished frozen sea which existed over wide stretches of the modern boreal land mass and which has kept the faunas on either side unique and largely unmixed. These results also suggest that the biological impacts of potential future ice sheet collapse promoted by human-induced climate change^{31,32} will require consideration of landscape dynamics across at least 15,000 year intervals.

Limitations of the study

Although the models were created based on more than 8,900 verified occurrences, for some species, occurrence data are still missing from some areas of their distribution. This could potentially impact model accuracy and some of our statistics. However, given the number of modeled species and robustness of the results, it is unlikely that this would change the general conclusions of the study. The use of LGM fossil records to parameterize multitemporal niche models was limited to ~1/3 of species. These tend to be marked calciphiles limited to wetland environments. The remaining taxa tend to occur in neutral/acidic soil conditions from mesic to xeric habitats. The only way that this latter component of the fauna could be considered here was by generating their LGM climate envelopes using only modern occurrences. Clearly this is only a rough approximation which does not allow for temporal changes in their niche-response. However, given that projections of unitemporal niches generated the same general trends as multitemporal (Figure S2), we assume that the patterns identified here are robust to this issue. However, if upland, acid-tolerant species possess differential temporal niche dynamics as compared to lowland calciphiles our estimates of range dynamics for the former could be in error.

RESOURCE AVAILABILITY

Lead contact

Further information and any requests should be directed to and will be fulfilled by the lead contact, Michal Horsák (horsak@sci.muni.cz).

Materials availability

This study did not generate new unique reagents.

Data and code availability

- All original source data and used publicly available data underlying this article are listed in the [key resources table](#). The data generated by our analysis can be found in [Data S1](#).
- R code for the estimation of species modern and LGM ranges has been deposited at GitHub and is publicly available as listed in the [key resources table](#).
- Any additional information required to reanalyze the data reported in this paper is available from the [lead contact](#) upon request.

Additional resources

Additional resources are provided in the supplemental information.

ACKNOWLEDGMENTS

We wish to thank Brian Coles, Stefan Meng, the National Museum of Wales, the Canadian National Museum, the Royal Ontario Museum, and the University of Michigan Museum of Zoology for access to their collections and willingness to let us verify specimen identifications. We are very grateful to Thomas A. Neubauer and an anonymous reviewer for providing useful comments to the first draft. This study was financially supported by the Czech Science Foundation projects P504/20-18827S and P504/23-05132S.

AUTHOR CONTRIBUTIONS

J.C.N. conceived the research, designed the study, collected field data, conducted statistical analyses, and wrote the manuscript; J.D. designed the study, conducted niche modeling, and assisted in manuscript preparation; M.H. conceived the research, designed the study, collected field data, and assisted in manuscript preparation.

DECLARATION OF INTERESTS

The authors declare no competing interests.

STAR★METHODS

Detailed methods are provided in the online version of this paper and include the following:

- [KEY RESOURCES TABLE](#)
- [METHOD DETAILS](#)
 - Input data
 - Climate niche modeling
 - Range and barrier characterization

- QUANTIFICATION AND STATISTICAL ANALYSIS
 - Range size and overlap
 - Barrier widths and types

SUPPLEMENTAL INFORMATION

Supplemental information can be found online at <https://doi.org/10.1016/j.isci.2024.111272>.

Received: August 13, 2024

Revised: September 30, 2024

Accepted: October 24, 2024

Published: October 28, 2024

REFERENCES

1. Nekola, J.C., and White, P.S. (1999). Distance decay of similarity in biogeography and ecology. *J. Biogeogr.* **26**, 867–878.
2. White, P.S., and Nekola, J.C. (1992). Biological diversity in an ecological context. In *Air Pollution and Biodiversity*, J.R. Barker and D.T. Tingey, eds. (Van Nostrand Reinhold), pp. 10–29.
3. Nekola, J.C., and White, P.S. (2002). Conservation, the two pillars of ecological explanation, and the paradigm of distance. *Nat. Area J.* **22**, 305–310.
4. Nekola, J.C., Divišek, J., and Horsák, M. (2022). The nature of dispersal barriers and their impact on regional species pool richness and turnover. *Global Ecol. Biogeogr.* **31**, 1470–1500.
5. Davis, M.B. (1984). Climatic instability, time lags, and community disequilibrium. In *Community Ecology*, J. Diamond and T.J. Case, eds. (Harper and Row), pp. 269–284.
6. Imbrie, J., Berger, A., Boyle, E.A., Clemens, S.C., Duffy, A., Howard, W.R., Kukla, G., Kutzbach, J., Martinson, D.G., McIntyre, A., et al. (1993). On the structure and origin of major glaciation cycles. II. The 100,000 year cycle. *Paleoceanography* **8**, 699–735.
7. Batchelor, C.L., Christie, F.D.W., Ottesen, D., Montelli, A., Evans, J., Dowdeswell, E.K., Bjarnadóttir, L.R., and Dowdeswell, J.A. (2023). Rapid, buoyancy-driven ice-sheet retreat of hundreds of metres per day. *Nature* **617**, 105–110.
8. Somveille, M., Manica, A., and Rodrigues, A.S.L. (2020). Simulation-based reconstruction of global bird migration of the past 50,000 years. *Nat. Commun.* **11**, 801.
9. Delcourt, P.A., and Delcourt, H.R. (1987). Long-term Forest Dynamics of the Temperate Zone. *Ecological Studies*, **63** (Springer-Verlag).
10. Ricklefs, R.E., and Schuler, D. (1993). Species diversity: regional and historical influences. In *Species Diversity in Ecological Communities* R. E. Ricklefs and D. Schuler, eds. (University of Chicago Press), pp. 350–364.
11. Nekola, J.C. (2014). North American terrestrial gastropods through either end of a spyglass. *J. Molluscan Stud.* **80**, 238–248.
12. Barker, G.M. (2001). Gastropods on land: phylogeny, diversity and adaptive morphology. In *The Biology of Terrestrial Molluscs* G. M. Barker, ed. (CABI Publishing), pp. 1–139.
13. Némec, T., Líznavá, E., Birkhofer, K., and Horsák, M. (2021). Stable isotope analysis suggests low trophic niche partitioning among co-occurring land snail species in a floodplain forest. *J. Zool.* **313**, 297–306.
14. Ložek, V. (1964). Quartärmollusken der Tschechoslowakei. (Rozpravy Ustředního ústavu geologického 31).
15. Shimek, B. (1913). The significance of Pleistocene mollusks. *Science* **37**, 501–509.
16. Horsáková, V., Nekola, J.C., and Horsák, M. (2020). Integrative taxonomic consideration of the Holarctic *Euconulus fulvus* group of land snails (Gastropoda, Stylommatophora). *Syst. Biodivers.* **18**, 142–160.
17. Nekola, J.C., Chiba, S., Coles, B.F., Drost, C.A., Horsák, M., and Horsák, M. (2018). A phylogenetic overview of the genus *Vertigo* O. F. Müller, 1773 (Gastropoda: Pulmonata: Pupillidae: Vertigininae). *Malacologia* **62**, 21–161.
18. Nekola, J.C., Coles, B.F., and Horsák, M. (2015). Species assignment in *Pupilla* (Gastropoda: Pulmonata: Pupillidae): integration of DNA-sequence data and conchology. *J. Molluscan Stud.* **81**, 196–216.
19. Gittenberger, E., Groenenberg, D.S.J., Kokshoorn, B., and Preece, R.C. (2006). Molecular trails from hitch-hiking snails. *Nature* **439**, 409.
20. Horsák, M., Ortiz, D., Nekola, J.C., and Van Bocxlaer, B. (2024). Intercontinental dispersal and niche fidelity drive 50 million years of global diversification in *Vertigo* land snails. *Global Ecol. Biogeogr.* **33**, e13820.
21. Cameron, R. (2016). *Slugs and Snails*. Collins New Naturalist Library, Book 133 (HarperCollins).
22. Barker, G.M., and Mayhill, P.C. (1999). Patterns of diversity and habitat relationships in terrestrial mollusc communities of the Pukeamaru Ecological District, northeastern New Zealand. *J. Biogeogr.* **26**, 215–238.
23. Nekola, J.C. (2010). Acidophilic terrestrial gastropod communities of North America. *J. Molluscan Stud.* **76**, 144–156.
24. Arbogast, B.S., and Kenagy, G.J. (2008). Comparative phylogeography as an integrative approach to historical biogeography. *J. Biogeogr.* **28**, 819–825.
25. Hewett, G. (2000). The genetic legacy of the Quaternary ice ages. *Nature* **405**, 907–913.
26. Weir, J.T., and Schluter, D. (2004). Ice sheets promote speciation in boreal birds. *Proc. Biol. Sci.* **271**, 1881–1887.
27. Weir, J.T., Haddrath, O., Robertson, H.A., Colbourne, R.M., and Baker, A.J. (2016). Explosive ice age diversification of kiwi. *Proc. Natl. Acad. Sci. USA* **113**, E5580–E5587.
28. Klicka, J., and Zink, R.M. (1997). Importance of recent ice ages in speciation: a failed paradigm. *Science* **277**, 1666–1669.
29. Gowan, E.J., Zhang, X., Khosravi, S., Rovere, A., Stocchi, P., Hughes, A.L.C., Gyllencreutz, R., Mangerud, J., Svendsen, J.-I., and Lohmann, G. (2021). A new global ice reconstruction for the past 80,000 years. *Nat. Commun.* **12**, 1199.
30. Graham, C.H., Moritz, C., and Williams, S.E. (2006). Habitat history improves prediction of biodiversity in rainforest fauna. *Proc. Natl. Acad. Sci. USA* **103**, 632–636.
31. Armstrong McKay, D.I., Staal, A., Abrams, J.F., Winkelmann, R., Sakschewski, B., Loriani, S., Fetzner, I., Cornell, S.E., Rockström, J., and Lenton, T.M. (2022). Exceeding 1.5 °C global warming could trigger multiple climate tipping points. *Science* **377**, eabn7950.
32. Khan, S.A., Choi, Y., Morlighem, M., Rignot, E., Helm, V., Humbert, A., Mouginot, J., Millan, R., Kjær, K.H., and Bjørk, A.A. (2022). Extensive inland thinning and speed-up of Northeast Greenland Ice Stream. *Nature* **611**, 727–732.
33. Kerney, M. (1999). *Atlas of the Land and Freshwater Molluscs of Britain and Ireland* (Harley Books).
34. Waldén, H. (2007). *Svensk landmolluskatlas* (Naturcentrum AB).
35. Haase, D., Fink, J., Haase, G., Ruske, R., Pécsi, M., Richter, H., Altermann, M., and Jäger, K.D. (2007). Loess in Europe—its spatial distribution based on a European Loess Map, scale 1:2,500,000. *Quat. Sci. Rev.* **26**, 1301–1312.
36. Pigati, J.S., McGeehin, J.P., Muhs, D.R., Grimley, D.A., and Nekola, J.C. (2015). Radiocarbon dating loess deposits in the Mississippi Valley using terrestrial gastropod shells (Polygyridae, Helicinidae, Discidae). *Aeolian Res.* **16**, 25–33.
37. Nekola, J.C., and Horsák, M. (2022). The impact of statistically unchallenged taxonomic concepts on ecological assemblages across multiple spatial scales. *Ecography* **2022**, e06063.
38. Nekola, J.C., and Coles, B.F. (2010). Pupillid land snails of eastern North America. *Am. Malacol. Bull.* **28**, 29–57.
39. Nekola, J.C., Hutchins, B.T., Schofield, A., Najev, B., and Perez, K.E. (2019). Caveat Consumptor Notitia Museo: let the museum data user beware. *Global Ecol. Biogeogr.* **28**, 1722–1734.
40. Meier, R., and Dikow, T. (2004). Significance of specimen databases from taxonomic revisions for estimating and mapping the global species diversity of invertebrates and repatriating reliable specimen data. *Conserv. Biol.* **18**, 478–488.
41. Hubricht, L. (1985). The distributions of the native land mollusks of the eastern United States. *Fieldiana New Series* **24**, 1–191.

42. Welter-Schultes, F.W. (2012). European non-marine molluscs, a guide for species identification (Planet Poster Editions).
43. Frest, T.J., and Dickson, J.R. (1986). Land Snails (Pleistocene-Recent) of the Loess Hills: A Preliminary Survey. *Proc. Iowa Acad. Sci.* 93, 130–157.
44. Haase, M., Meng, S., and Horsák, M. (2021). Tracking parallel adaptation of shell morphology through geological times in the land snail genus *Pupilla* (Gastropoda: Stylommatophora: Pupillidae). *Zool. J. Linn. Soc.* 191, 720–747.
45. Pigati, J.S., Rech, J.A., and Nekola, J.C. (2010). Radiocarbon dating of small terrestrial gastropod shells in North America. *Quat. Geochronol.* 5, 519–532.
46. Grimley, D.A., Larsen, D., Kaplan, S.W., Yansa, C.H., Curry, B.B., and Oches, E.A. (2009). A multi-proxy palaeoecological and palaeoclimatic record within full glacial lacustrine deposits, western Tennessee, USA. *J. Quat. Sci.* 24, 960–981.
47. Horsák, M., Juříčková, L., Škodová, J., and Ložek, V. (2016). *Pupilla alluvionica* Meng & Hoffmann, 2008: a land snail extant in the Altai refugium recognised for the first time in Central European Early-Middle Pleistocene glacials. *Malacologia* 59, 223–230.
48. Hijmans, R.J., Cameron, S.E., Parra, J.L., Jones, P.G., and Jarvis, A. (2005). Very high resolution interpolated climate surfaces for global land areas. *Int. J. Climatol.* 25, 1965–1978.
49. Title, P.O., and Bemmels, J.B. (2018). ENVIREM: an expanded set of bioclimatic and topographic variables increases flexibility and improves performance of ecological niche modeling. *Ecography* 41, 291–307.
50. Castellanos, A.A., Huntley, J.W., Voelker, G., and Lawing, A.M. (2019). Environmental filtering improves ecological niche models across multiple scales. *Methods Ecol. Evol.* 10, 481–492.
51. Phillips, S.J., Anderson, R.P., Dudík, M., Schapire, R.E., and Blair, M.E. (2017). Opening the black box: An open-source release of Maxent. *Ecography* 40, 887–893.
52. Phillips, S.J., and Dudík, M. (2008). Modeling of species distributions with Maxent: new extensions and a comprehensive evaluation. *Ecography* 31, 161–175.
53. Phillips, S.J., Dudík, M., Elith, J., Graham, C.H., Lehmann, A., Leathwick, J., and Ferrier, S. (2009). Sample selection bias and presence-only distribution models: implications for background and pseudo-absence data. *Ecol. Appl.* 19, 181–197.
54. Hirzel, A.H., LeLay, G., Helfer, V., Randin, C., and Guisan, A. (2006). Evaluating the ability of habitat suitability models to predict species presences. *Ecol. Modell.* 199, 142–152.
55. Hurlbert, A.H., and White, E.P. (2005). Disparity between range map and survey based analyses of species richness: patterns, processes and implications. *Ecol. Lett.* 8, 319–327.
56. Svenning, J.-C., and Skov, F. (2004). Limited filling of the potential range in European tree species. *Ecol. Lett.* 7, 565–573.
57. Nekola, J.C. (1999). Paleoreugia and neoreugia: the influence of colonization history on community pattern and process. *Ecology* 80, 2459–2473.
58. Carcaillet, C., Latil, J.-L., Abou, S., Ali, A., Ghaleb, B., Magnin, F., Roiron, P., and Aubert, S. (2018). Keep your feet warm? A cryptic refugium of trees linked to a geothermal spring in an ocean of glaciers. *Glob. Chang. Biol.* 24, 2476–2487.
59. Jacquemyn, H., Brys, R., and Hermy, M. (2002). Patch occupancy, population size and reproductive success of a forest herb (*Primula elatior*) in a fragmented landscape. *Oecologia* 130, 617–625.

STAR★METHODS

KEY RESOURCES TABLE

REAGENT or RESOURCE	SOURCE	IDENTIFIER
Biological samples		
Coordinates of modern occurrence records used in Maxent models	Our personal collections; the Brian Coles collection at the National Museum of Wales; University of Michigan Museum of Zoology; Royal Ontario Museum; National Museum of Canada; Kerney (1999) ³³ ; Waldén (2007) ³⁴	Data S5
Coordinates of LGM quasi-occurrence records used in multitemporal Maxent models	This paper	Data S6
Deposited data		
Climate data for modern and LGM periods	WorldClim 1.4	https://www.worldclim.org/data/v1.4/worldclim14.html
Climate data for modern and LGM periods	ENVIREM	https://envirem.github.io/
Software and algorithms		
R code for the estimation of species modern and LGM ranges	This paper	https://github.com/jdivisek/LGMlegacy
Maxent version 3.4.4.	https://biodiversityinformatics.amnh.org/open_source/maxent/	https://github.com/mrmxent/Maxent
Other		
Loess map of Europe	Haase et al. (2007) ³⁵	https://doi.org/10.1016/j.quascirev.2007.02.003
Loess map of the Mississippi Valley	Pigati et al. (2015) ³⁶	https://doi.org/10.1016/j.aeolia.2014.10.005

METHOD DETAILS

Input data

Study organisms

We have chosen to investigate small (shell dimension <5 mm) Holarctic land snails from the genera *Euconulus*, *Pupilla* and *Vertigo* that have been validated by integrative taxonomic revisions.^{16–18} This is essential given that traditional taxonomic concepts had a 50% error rate arising from oversplitting, overlumping, and/or the use of incorrect identification features.³⁷ Use of occurrence records based on such inaccurate concepts would have incorporated error rates ranging from +75% to –50% into species-specific polygon areas in 2D climate PCA space.⁴ We only considered entities whose range centers are at least 40°N in eastern Eurasia and central/eastern North America and 50°N in central/western Eurasia. This difference stems from a shifting of boreal species ranges north due warmer winter temperatures at similar latitudes in western Eurasia from Gulf Stream maritime influence. We assigned each species into one of three biogeographic affinities based on their median longitude: European (26°W–60°E), Beringian, including also areas east of the Urals (60°E–133°W), and North American (133°W–26°W). Additional specific criteria are found in the Supplementary Materials.

Modern occurrences

Using genetically-validated diagnostic shell traits,^{16–18} all occurrences within our personal collections and from the Brian Coles collection at the National Museum of Wales were reverified. We also reidentified all Holarctic *Pupilla* and *Vertigo* lots from the University of Michigan Museum of Zoology, Royal Ontario Museum and National Museum of Canada.³⁸ For species that possess easily observed and robust diagnostic features we have also incorporated mapped occurrence data from the UK/Ireland³³ and Sweden.³⁴ Given that unvalidated museum land snail records possess a 20% misidentification rate,³⁹ and that online database identifications in other invertebrate groups possess error rates up to 80%,⁴⁰ we have chosen to ignore such data as we have no way to verify identifications or generate *a priori* rules regarding which reports to exclude. Our preference is to parameterize climate envelope models using smaller but higher-quality data. Through this process over 8900 individual occurrence records were accumulated. These observations span the full known geographic, ecological, and climatic ranges of each species.^{16,17,38,41,42}

Fossil occurrences

Eighteen species possess identifiable LGM fossils.^{14,15,41,43–45} Since known fossil sites are much fewer than modern occurrences, generation of multitemporal niche envelopes using only reported fossil occurrences would down-weight their contribution to the final model. They would also likely introduce bias from any non-random climate occurrence of taphonomically appropriate deposits. We have attempted to correct for this by first mapping the known LGM fossil range of each species. Because the overwhelming majority of fossil occurrences in both Europe and North America are associated with loess deposits,^{14,15,46} we obtained loess coverage maps^{35,36} and randomly selected an equal number of quasi-occurrences as pruned modern occurrences (Data S5, see below) from the region of overlap. The quasi-occurrences for each species (Data S6) are mapped in Data S1.

Refinement of analyzed taxa list

Pupilla hebes was included for analysis even though its range center lies south of our normal range because it is limited to montane taiga. We did not model *V. aff. hoppi* because we are currently unable to distinguish it based on shell features alone and know of only four genetically-confirmed sites. Additionally, because of lingering ambiguity regarding taxonomic status,¹⁷ we have chosen to lump *V. ronneyensis* + *V. ultimathule* and to lump *V. coloradensis* + *V. cristata* + *V. pisewensis*. We treated as distinct the western North American populations of *Euconulus alderi* and the eastern Eurasian and North American populations of *Vertigo lilljeborgi* because of their unique sequence signatures in combination with geographic isolation. The only reason these entities have not yet been formally described as distinct species is that there are not yet enough known sites and material to accurately demarcate their genetic/morphological variability and geographic range. Additionally, because each also possesses fewer than five known populations, we could not separately model their climate envelopes. To include them in this analysis we have lumped their occurrence records into *E. alderi* or *V. lilljeborgi*, respectively. This approach appears justified as the resultant suitability models accurately portrayed not only the known ranges of these species but their better-known European relatives as well. Species with five or fewer known modern occurrences (*P. limata*, *V. binneyana*, *V. chytryi*) were not modeled. *Pupilla alluvionica*, although having 14 known occurrences, was also not modeled as its extreme spatial limitation and climatic homogeneity among known sites⁴⁷ limits reliability of global-scale interpolation. We have chosen to not generate multitemporal models for *Vertigo oughtoni*, which has been reported as LGM fossil,^{41,43} because its traditional diagnosis was based on faulty shell identification features leading to confusion with at least two other species. As a result its reported fossil sites cannot be trusted, making the generation of accurate climatic niches impossible.

Climate

At each modern occurrence, we retrieved 35 climatic variables at a resolution of 5 arc-minutes from the WorldClim v.1.4⁴⁸ and ENVIREM⁴⁹ databases. We pruned these to avoid potential bias caused by uneven occurrence record density⁵⁰: for species with more than 80 occurrences, each occurrence was placed into a multidimensional Principal Components Analysis (PCA) space, with the number of axes representing the number needed to capture at least 90% of observed variation in climatic variables. We then randomly removed one of the occurrence records associated with the smallest distance pair. This process was repeated until all remaining pairwise distances were 0.1 standard deviations or greater, or the number of records reached 80, whichever came first. The number of records used to calibrate each climate envelope model is provided in Data S3; with the pruned records provided in Data S5 and also mapped in Data S1.

For the 18 species possessing identifiable LGM fossils, we recorded values from each quasi-occurrence for the same 35 climatic variables at ~22 ka BP from the simulations of MPI-ESM-P, CCSM4, and MIROC-ESM global circulation models. Given that loess was deposited over tens of thousands of years during the last glacial cycle, considering climate at only this single time is obviously highly approximate. However, this seems reasonable given it represents the harshest climate corresponding to the period of greatest loess deposition.³⁶

Climate niche modeling

We used Maxent 3.4.4⁵¹ to model species-specific suitable climates because it uses presence-only data and generally performs well across all sample sizes.⁵² Unitemporal models considered only modern climate from pruned occurrences (Data S5). For species with LGM quasi-occurrences, a multitemporal model was created from each LGM global climate simulation. All models used 10000 background points randomly assigned within well-surveyed regions defined by a minimum convex envelope extending 100 km beyond the most marginal occurrences in our dataset.⁵³ To control for multicollinearity, we limited calibration to a species-specific subset of the best performing variables. This was determined by calibrating single-variable Maxent model models for each species. The performance of each was documented using Area Under a ROC Curve (AUC) scores, and ranked from best to worst. The two best-performing variables were selected, and if their Variance Inflation Factor (VIF) was lower than 10, the third best-performing variable was added to the subset and collinearity again checked. This process was repeated until VIF of all variables in the subset exceeded 10.

Climate suitability was then calculated by projecting each model into modern or LGM Holarctic landscapes. A single LGM projection was generated by calculating the mean across the three paleoclimate projections. All models were evaluated using 5-fold cross-validation. Four metrics were utilized: (1) AUC; (2) Overfitting; (3) maximum True Skill Statistics; and (4) Continuous Boyce Index.⁵⁴ We tested the ability of unitemporal and multitemporal models to predict LGM fossil ranges by recalculating the Continuous Boyce Index for 100 samples each representing 100 randomly selected LGM quasi-occurrences.

Potential modern and LGM range of each species was estimated by applying the Maxent “Balance” threshold (which minimizes $6 \times$ training omission rate + $0.04 \times$ cumulative threshold + $1.6 \times$ fractional predicted area) with areas above this threshold being considered

climatically suitable. Holarctic-wide maps of potential ranges for each species in both the modern and LGM were then generated (Data S1). These range estimates are near the theoretical maximum as species never fully occupy their full potential ranges.^{55,56} Additionally, species occurrences at range margins often represent microclimatically unique habitats – such as cooled air emanating from ice caves⁵⁷ or warm air associated with geothermal fields.⁵⁸ For purposes of the following analyses, we assume that the occupied-to-potential range ratio does not significantly vary between the LGM and modern.

To address potential uncertainty arising from the choice of modeling algorithm, we additionally fitted models using Random Forest (RF) and Generalized Linear Model (GLM) algorithms and combined these with Maxent to generate an ensemble prediction. The statistical patterns present in ensemble-derived ranges were found to exactly correspond to Maxent-only analyses (Table S3; Figures S3 and S4). Combined with the fact that some ensemble projections appeared biogeographically unreasonable, we opted to only analyze outcomes derived from the less complex Maxent approach.

Range and barrier characterization

Range measurement and extent

LGM-to-modern distribution for each species was determined across nine roughly equal-sized Holarctic regions to quantize constant environmental variability: western (Region 1: west Greenland shore–7°E), central (Region 2; 7°E–35°E) and eastern (Region 3, 35°E–60°E) Europe; western (Region 4, 60°E–110°E), central (Region 5, 110°E–163°E), and eastern (Region 6, 163°E–133°W) Beringia; and western (Region 7, 133°W–102°W), central (Region 8, 102°W–79°W) and eastern (Region 9, 79°W–Labrador/Baffin Island) North America (Figure 1B). This was done by first noting from which regions a given species is currently known to reside. We then added regions which harbored LGM fossils. The potential total range area and size of the largest contiguous patch in both the LGM and modern was determined from each occupied region. The amount of modern range area which overlapped LGM range was also calculated (Data S3).

Dispersal barrier measurement

The type and width of range barriers was recorded both to the east and west of modeled range limits in the LGM and modern. This requires identification of unoccupied areas possessing appropriate climate of minimally-sufficient area, as the simple presence of an appropriate 5 arc-minute climate pixel does not indicate expected population existence. Because population colonization and persistence are unlikely when total appropriate area and largest patch size is too small⁵⁹ we have recorded regions possessing little potential climate as being inappropriate. Using actual modern Holarctic species occurrences as a guide, we set these lower thresholds at a total regional area of 90000 km² with a maximum patch size of 45000 km². Distances between occupied and unoccupied areas were then calculated as straight-line routes that did not exceed 70°N; e.g., transpolar routes were disallowed. The principle mechanism (inappropriate climate, ocean or ice sheet) underlying each barrier was also recorded. If more than one appeared responsible, each was noted. An example is provided in Figure 1B. When actual range was found to terminate significantly (e.g., 1500+ km) before the end of a predicted range, barrier width was recorded as missing with habitat/history being recorded as the barrier type. In addition, if the southern modern range terminus was farther north than the northern LGM range terminus, we calculated the distance separating them within each occurrence region. The resultant data matrix across all species is provided in Data S4.

QUANTIFICATION AND STATISTICAL ANALYSIS

Range size and overlap

Changes in appropriate total predicted range and maximum patch size per occupied region were illustrated using a histogram, with significance being estimated using a Paired Wilcoxon Signed Rank test (Figures 2, S1, and S3). Changes in total predicted range across all taxa from LGM-to-modern within all nine regions was illustrated using a box-plot with significance being estimated using the Kruskal-Wallis test (Figures 3, S2, and S4). The number of species that demonstrated overlap between LGM and modern ranges was determined across the three biogeographic affinities as well as the nine regions. Significance was estimated using Fisher's Exact test (Table 2, S1, and S3).

Barrier widths and types

A histogram was generated showing changes in all non-zero barrier widths between the LGM and modern, with significance being estimated using a Paired Wilcoxon Signed Rank test (Figure 2, S1, and S3). The significance of observed variation in the number of barriers associated with oceans, inappropriate climate, ice sheets, and history/ecology between the LGM and modern across the three biogeographic affinities and nine regions was estimated using Fisher's Exact test (Table 2, S1, and S3).